BUCKLING OF REINFORCING BARS IN CONCRETE STRUCTURES UNDER SEISMIC LOADS

Zhiyu Zong[1] and Sashi Kunnath[2]

[1] *Ph.D. Candidate, Dept. of Civil and Environmental Engineering, University of California, Davis, USA*
[2] *Professor, Dept. of Civil and Environmental Engineering, University of California, Davis, USA*
Email: zzong@ucdavis.edu, skkunnath@ucdavis.edu

ABSTRACT:

The objective of this research is to develop a simple and reliable constitutive model for reinforcing steel bars which includes the effects of bar buckling for use in nonlinear seismic analysis of reinforced concrete (RC) structures. Bar buckling is an important phenomenon in the post-elastic response of RC columns subjected to seismic loads. To facilitate this development, a series of nonlinear finite element simulations were carried out to identify the main parameters controlling the buckling behavior of reinforcing bars. In the first set of simulations, individual bars with varying length to cross-sectional diameter (L/D) ratios were considered while in the second phase full column models with varying longitudinal and transverse reinforcement were simulated. In both cases, the specimens were subjected to axial compressive loading to observe the post-buckling response of the longitudinal bars. Numerical simulations are compared to experimental results and findings from the study provide a basis for developing a new material model for reinforcing steel bars in RC columns.

KEYWORDS: analysis, buckling, constitutive model, reinforced concrete

1. INTRODUCTION

In reinforced concrete columns subjected to seismic loads, failure is often initiated by buckling of the longitudinal bars. For reliable simulation of the nonlinear response of RC structures, a proper material model for reinforcing bars with the effects of buckling is essential. Previous studies, both analytically and experimentally, have focused on different aspects of bar buckling and its impact on structural response. Mau (1990) and Mau and El-Mabsout (1989) developed a beam-column element for the finite element inelastic buckling analysis to determine the column load-carrying capacity. Pantazopoulou (1998) compiled data from the literature of over 300 column tests and developed requirements for reinforcement stability that recognize the interaction between displacement ductility demand in critical section, tie effectiveness, limiting concrete strain, bar size and tie spacing. Dhakal and Maekawa (2002a) used fiber finite element analyses to present an average compressive stress-strain relation for reinforcing bars as a function of slenderness ratio and yield strength. Later, Bae et al. (2005) conducted an experimental program study on bar buckling and examined the effects of three important bar parameters, the L/D ratio (length over bar diameter), e/D (initial imperfection over bar diameter) ratio and the ratio of ultimate strength to yield strength. Dhakal and Maekawa (2002b) derived a method to predict the buckling length of longitudinal reinforcing bars using an energy method. The authors pointed out that the assumption, widely adopted by previous researchers, that the buckling length of longitudinal reinforcement bars inside an RC member is equal to the spacing of lateral ties is not true.

From the literature review, it is clear that many issues related to the prediction of buckling behavior of bars in reinforced concrete columns remain unresolved due to lack of sufficient data and reliable models. Additional research is needed on the parameters influencing buckling response of bars in reinforced concrete columns, such as effective buckling length, interactions between longitudinal bars, hoops and concrete, as well as the development of average bar constitutive relations. This study aims to provide additional insight into bar buckling behavior and proposes a basis for developing a constitutive model for reinforcing steel which incorporates the effect of buckling.

2. SINGLE BAR MODEL

2.1. Model description

Three dimensional finite element single bar models were built using the commercial software LS-DYNA as shown in Figure 1. Solid elements, which include 6 node pentahedrons and 8 node hexahedrons, are adopted to represent a typical reinforcing steel bar. The steel material model used for the simulations is a simple bilinear model with kinematic hardening and these properties are based on the experimental results reported by Bae et al. (2005) . All the nodes at the two ends of the bar are fixed in all three rotational degrees of freedom and two translational degrees of freedom except for the axial direction (global z direction as shown in Figure 1). Axial displacement control along the axial direction is imposed to obtain the buckling response of the bar.

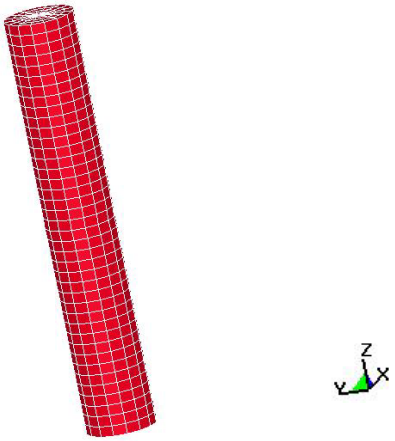

Figure 1 FE model of single reinforcing bar

Table 1 Material properties for single bar model

Material type	Kinematic hardening plasticity
Young's Modulus (Pa)	2.0E11
Yield stress (Pa)	4.37E8
Post-yield modulus (Pa)	3.0E9 (1.5% E_s)
Poisson's ratio	0.3

2.2. Average stress-strain relationship including buckling

The single bar model with different length over bar diameter ratios (L/D) were subjected to axial compressive loading through imposed axial displacements and the average stress-strain relationship of the bars were simulated. For a single bar with a certain type of material, the stress-strain response depends on the L/D ratio of the bar. For different L/D ratios, the average stress-strain curves in compression are shown in Figure 2. The computed stress-strain relationship of each bar with varying L/D ratio from 4.0 to 10.0 are compared with the experimental obtained results by Bae et al (Bae et al. 2005). The main parameter controlling the post-buckling behavior was found to be the post-yield modulus of the material. It is observed that reasonably good agreement with experiments is obtained with a post-yield modulus of 1.5% of the initial elastic modulus.

From the results presented in Figure 2, it is noted that the average stress-strain response for L/D=4 obtained from the LS-DYNA simulation model is significantly different from the experimentally obtained behavior. That is because when L/d is very small, buckling does not occur in the numerical model and the response simply represents the input stress-strain material property (which in this case is bilinear kinematic hardening, and not a realistic representation of steel property).

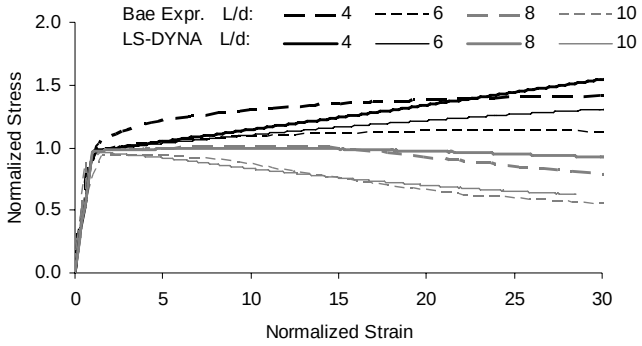

Figure 2 Average compressive stress-strain relationship computed using LS-DYNA and comparison with experimental results by Bae et al. (2005)

The specified strength of the reinforcing bar also influences the behavior in compression. Figure 3 shows the average stress-strain for bars with L/D=10 and yield strengths corresponding to 100MPa, 200MPa, 400MPa and 800MPa, respectively. The softening of average stress-strain response becomes steeper with the increase in yield strength for a particular slenderness (L/D) ratio.

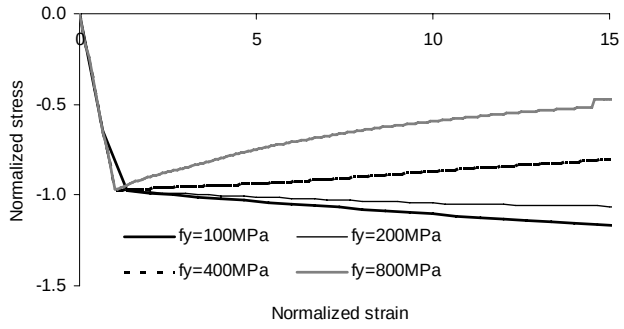

Figure 3 Normalized stress-strain response (L/D=10) for varying yield stress

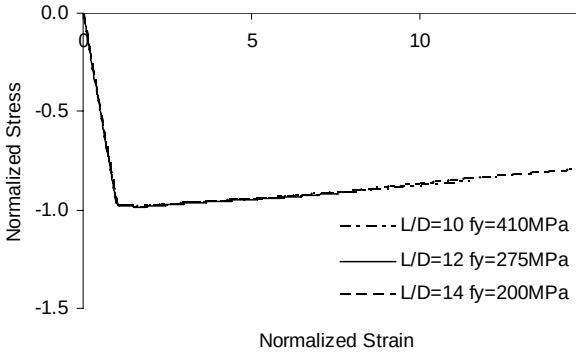

Figure 4 Identical normalized stress-strain curves for several L/D and yield strength combinations

In the next phase of the simulation study, the geometric and material properties (namely, L/D and yield strength) were combined to produce a single parameter. Following a series of simulations, it was established that for some L/D and yield strength combinations, the same normalized stress vs. strain curves were obtained. Numerous single bar models with L/D varying from 4 to 20 and yield stress varying from 200MPa to 600MPa were developed. By searching for identical constitutive curves and analyzing the parameters, it was found that the combined parameter $\sqrt{f_y}(L/D)$ produces similar average stress vs. strain curves. This conclusion agrees with some previous findings for single bar buckling analysis (Dhakal and Maekawa 2002a).

2.3. Effect of initial tension

In order to investigate the effects of tension on the initiation of bar buckling, the displacement histories as shown in

Figure 5 are imposed on the single bar models. All the four cases considered are based on similar displacement history sequence. Linear tensile displacements are first imposed on both ends of the model from time t=0 to time t=1 second, followed by unloading to zero displacement during the next 1.0 second and finally loading in tension up to buckling of the bar.

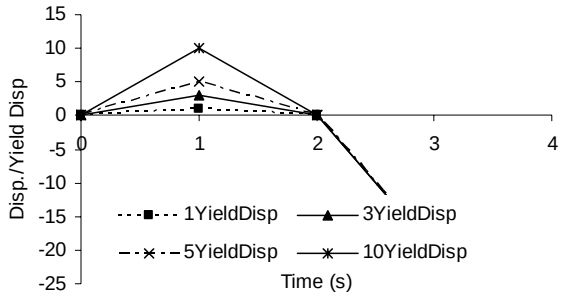

Figure 5 Displacement histories imposed on single bar model

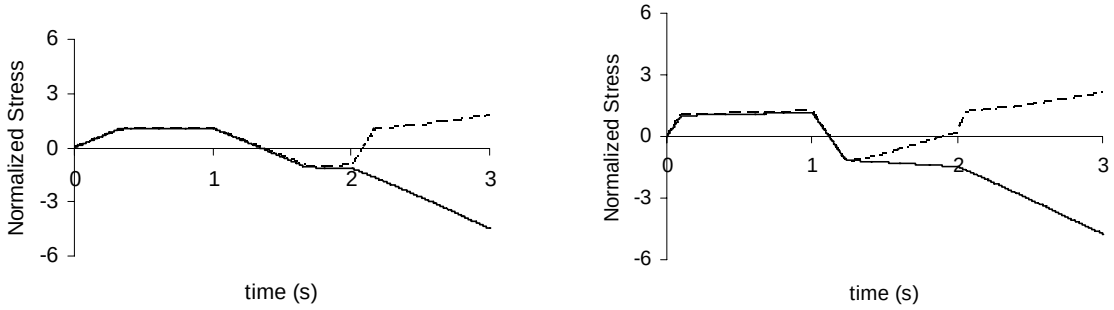

(a) (b)

Figure 6 Stresses on tensile (solid line) and compressive sides (dotted line) of buckling section
(a) Bar subject to initial tension of $3\varepsilon_y$ (b) Bar subject to initial tension of $10\varepsilon_y$

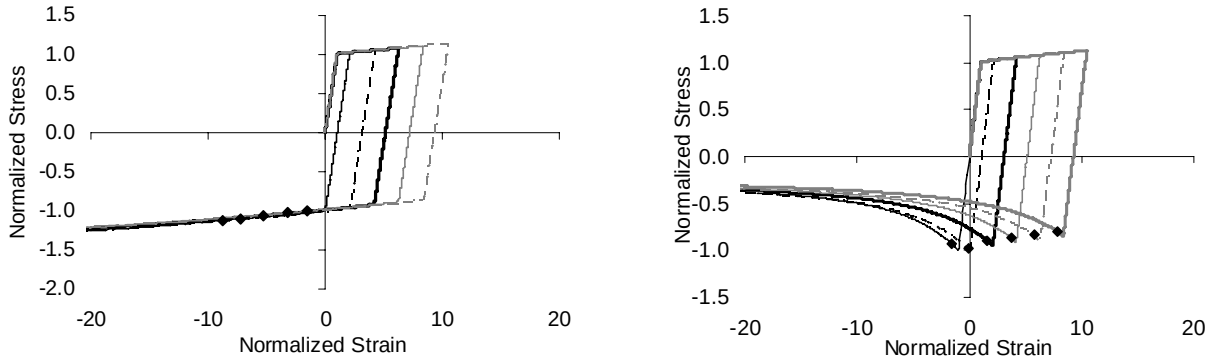

(a) (b)

Figure 7 Average stress-strain curves for #4 bar subjected to varying levels ($2\varepsilon_y$ to $10\varepsilon_y$) of initial tension
(a) L/d = 6 (b) L/d = 15

Figure 6 displays the stresses at the concave and convex sides on the buckled sections for two cases. It is obvious that the preceding peak tension strain history does affect buckling initiation and development. Figure 7 shows the recorded average stress vs. strain for the different load cases for two L/d ratios. The black dots indicate the onset of buckling. The larger are the preceding tensile strains, the earlier the buckling is initiated. This finding is consistent with the results reported by Rodriguez et al. (1999).

3. FULL COLUMN MODELS

3.1. Model Description

Three dimensional finite element models of complete reinforced concrete columns as shown in Figure 8 were

developed using LS-DYNA (Hallquist 2003). The column model includes three parts: concrete, longitudinal reinforcing bars and transverse reinforcing steel. The concrete section was modeled using elastic solid elements while both the longitudinal reinforcing bars and transverse steel were modeled using beam elements (Belyschko-Schwer tubular beam with cross-section integration). The following constraints and boundary conditions are imposed on the model to generate a valid first mode buckling shape.

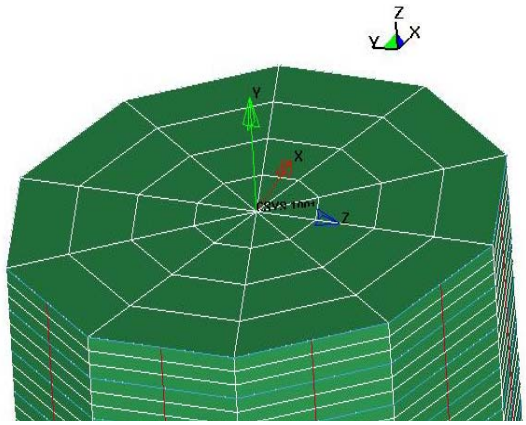

Figure 8 Three-dimensional finite element column model showing global and local coordinate system

*(1)*Longitudinal and transverse reinforcements share the same nodes at their intersections.

(2) Between the concrete surface and longitudinal rebar nodes, node-to-surface contact is defined to transfer force between the concrete and longitudinal rebar nodes.

*(3)*All the longitudinal rebar nodes are constrained to move only in radial directions of the cross section. As shown in Figure 8, in the specified local coordinates, movements in local y and x direction are free while the movements in local z direction (tangent direction) are fixed.

*(4)*The nodes assigned to concrete, longitudinal rebar and transverse reinforcement on the same cross section are constrained to move together in the global z direction.

(5) Translational displacement in global x and global y direction and all three rotational displacements are fixed for all nodes at the two ends.

(6) Displacement control is imposed in the global z direction on all nodes at the two ends.

3.2. Comparison with experimental results

To establish the adequacy of the model to simulate the interactions between the hoops, longitudinal reinforcing bars, and concrete, the simulated buckling shapes of typical columns were compared with experimentally available results since experimental data on the stress vs. strain relationship of longitudinal reinforcing bars were difficult to obtain. The numerically simulated buckling shape is compared to the experimentally observed shape reported by Calderone et al (2001) in Figure 9. The main properties of the column are listed in Table **2**. The comparison present in Figure 9 show that the finite element column models are able to simulate longitudinal bar buckling adequately, validating the ability of the finite element model to simulate the interaction between the hoops, longitudinal bars and concrete (note that the buckling occurs across 7 hoops).

Table 2 Properties of model column used in simulation (Calderone et al. 2001)

Material		**Longitudinal Reinforcement**	
Concrete Strength (MPa)	34.5	Diameter (Db) (mm)	19.0
Transverse Steel Yield Stress (MPa)	606.8	Number of Bars	28
Longitudinal Steel Yield Stress (MPa)	441.3	Reinforcement ratio (%)	2.73
Geometry		**Transverse Reinforcement**	
Section type	Circle	Diameter (Dh) (mm)	6.4
Diameterd (Dc) (mm)	609.6	Spacing (s) (mm)	25.4
		Reinforcement Ratio (%)	0.89

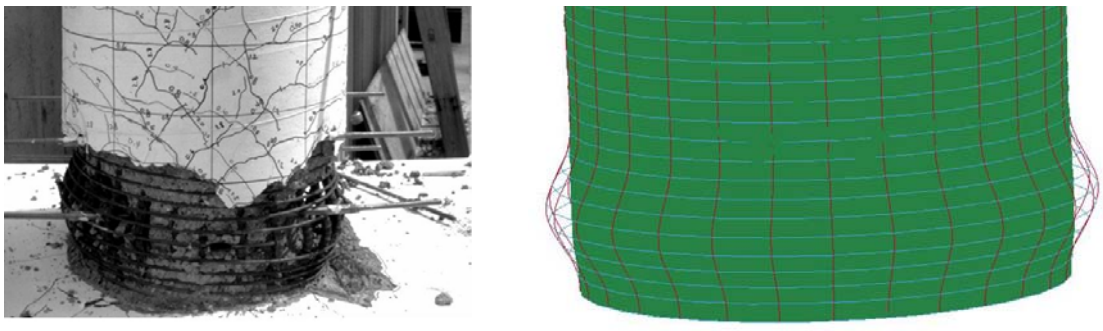

(a) (b)

Figure 9 Comparison of simulated and experimentally (Calderone et al. 2001) observed buckling shape
(a) experiment (b) simulation

4. SIMPLIFIED BAR-WITH-SPRINGS MODEL

To provide a simple analytical model to predict bar buckling behavior under seismic loads, a single longitudinal bar in a reinforced concrete column is simulated as a flexural member. The combined constraints resulting from the hoops, interior concrete, column size and longitudinal reinforcement arrangement are represented by springs at the hoop locations. This concept is shown schematically in Figure 10. Values of spring stiffness are developed based on the results of parametric simulations. The proposed procedure is applied to a typical column whose properties are summarized in Table 3.

Table 3 Properties of example column

Material		**Longitudinal Reinforcement**	
Concrete strength (MPa)	32.7	Diameter (Db) (mm)	29.07
Transverse steel yield stress (MPa)	420	Number of Bars	6
Longitudinal bar yield stress (MPa)	420	Reinforcement ratio (%)	1.2
Geometry		**Transverse Reinforcement**	
Section type	Circular	Diameter (Dh) (mm)	12.7
Diameter (Dc) (mm)	650	Spacing (s) (mm)	200
		Reinforcement Ratio (%)	0.39

The effective transverse stiffness of the hoops is estimated in two ways: by considering the force in either the hoops or the longitudinal bars. Results are presented in Figure 11 – and the similarity in the response indicates that the constraints imposed in the finite element model are reasonable. In order to establish the stiffness of the hoops for the bar-with-springs model, a single hoop from the column was extracted and radial forces were applied uniformly to simulate the behavior of the hoops when columns are subjected to axial compression. The force-deformation response from the single hoop model was evaluated and compared to the global responses determined from the full column model. The comparison is shown in Figure 11. It is seen that all three responses are nearly identical which indicates that it is possible to establish the stiffness of the spring (Figure 10) by examining the response of a single hoop with proper constraints. The comparisons with the force-deformation response obtained by considering the shear in the longitudinal bar and hoop reinforcement of the full column model validates the procedure. Hence, it is possible to develop the properties of the spring using a simple single hoop model.

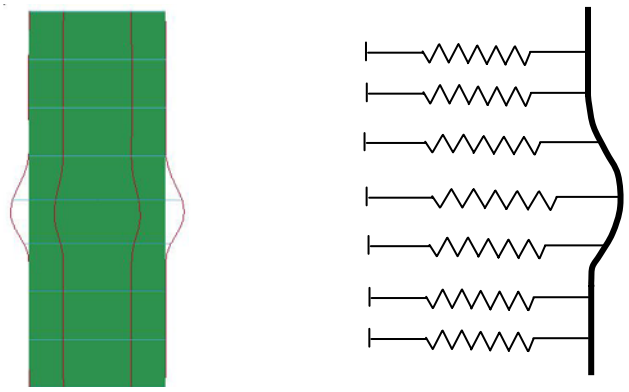

(a) (b)

Figure 10 Development of simplified model
(a) Full column FE model (b) Corresponding bar-with-springs model

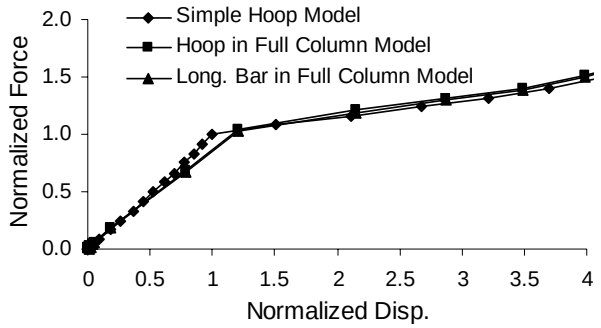

Figure 11 Effective transverse steel stiffness from column model and hoop model

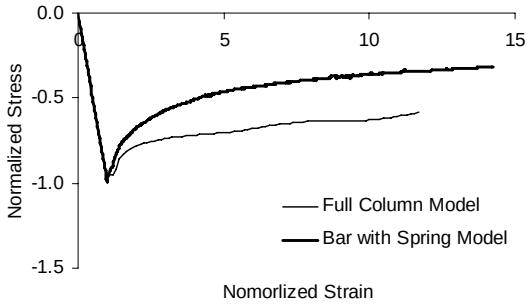

Figure 12 Comparison of stress vs. strain curves obtained from simplified spring model and full column finite element model

Numerous simulations from both full column models and bar with spring models were compared. It was demonstrated that both models result in similar buckling shapes. This provided further evidence that when proper constraints are applied to the longitudinal bars in the bar-with-springs model in conjunction with appropriate spring properties, it is possible to simulate bar buckling in actual RC columns.

Finally, the computed stress vs. strain relations from the full column models and the bar-with-springs models are compared in Figure 12. For larger strains, the stress provided by column model is greater than the stress computed with the simplified model. The difference may be a consequence of the extra constraints imposed on the column model which were required to obtain proper buckling shapes.

Therefore, the process of simulating constitutive stress-strain relationship of a longitudinal bar in compression becomes a two stage problem. First, we convert the complex full column FE model to a simple bar-with-springs model. The properties of springs combines the effects of rebar arrangement, column size, properties of transverse reinforcement, etc. The relationship for estimating effective spring properties is developed through curve fitting of numerical simulations. The second step is to impose axial forces in the simplified bar-with-springs model to develop average stress vs. strain relationships.

5. CONCLUSIONS

3D finite element models were developed in LS-DYNA to study bar bucking mechanism in both single bars and bars in embedded in reinforced concrete columns with transverse confinement. The effects of several significant parameters, such as length over bar diameter (L/D) ratio, material strength and initial tension were investigated to determinate the average stress vs. strain relations including buckling in single bars. Initial tension effects on buckling response analysis verified that preceding tensile strain does affect the onset of bar buckling. A detailed

comparative study indicated that full-column FE models can reasonably predict the interaction between the longitudinal bars, hoop reinforcement and core concrete and generate buckling shapes comparable to those obtained in experimental tests. To simplify the buckling analysis, a bar-with-springs model was developed. Spring properties were obtained from data fitting of numerical simulations and represent the combined effects of significant column parameters such as column size, longitudinal bar arrangement, and transverse steel properties. The approach presented by this paper provides a new methodology for generating the compressive stress-strain behavior of reinforcing bars including buckling.

ACKNOWLEDGEMENTS

This work was partially supported by the Earthquake Engineering Research Centers Program of the National Science Foundation under award number EEC-9701568 through the Pacific Earthquake Engineering Research Center (PEER). Any opinions, findings, and conclusion or recommendations expressed in this material are those of the authors and do not necessarily reflect those of the National Science Foundation.

REFERENCES

Bae, S., Mieses, A. M., and Bayrak, O. (2005). "Inelastic buckling of reinforcing bars." *Journal of Structural Enginerring*, **131(2)**, 314-321.

Berry, M. P., and Eberhard, M. O. (2005). "Practical performance model for bar buckling." *Journal of Engineering Mechanics*, **131(7)**, 1060-1070.

Calderone, A. J., Lehman, D. E., and Moehle, J. P. (2001). "Behavior of Reinforced Concrete Bridge Columns Having Varying Aspect Ratios and Varying Lengths of Confinement." University of Washington, Seattle.

Dhakal, R. P., and Maekawa, K. (2002a). "Modeling for postyield buckling of reinforcement." *Journal of Structural Engineering*, **128(9)**, 1139-1147.

Dhakal, R. P., and Maekawa, K. (2002b). "Reinforcement stability and fracture of cover concrete in reinforced concrete members." *Jounal of structural engineering*, **128(10)**, 1253-1262.

Freytag, D. M. (2006). "Bar buckling in reinforced oncrete bridge columns ", University of Washington.

Gomes, A., and Appleton, J. (1997). "Nonlinear cyclic stress-strain relationship of reinforcing bars including buckling." *Engineering Structures*, **19(10)**, 822-826.

Hallquist J.O. (2003). LS-DYNA keyword user's manual, Version 970. Livermore Software Technology Corporation, California.

Lehman, D., Moehle, J., Mahin, S., Calderone, A., and Henry, L. (2004). "Experimental evaluation of the seismic performance of reinforced concrete bridge columns." *Journal of Engineering Mechanics*, **130(6)**, 869-879.

Mau, S. T. (1990). "Effect of tie spacing on inelastic buckling of reinforcing bars." *ACI Structural Journal*, **87(6)**, 617-677.

Mau, S. T., and El-Mabsout, M. (1989). "Inelastic buckling of reinforcing bars." *Journal of Engineering Mechanics*, **115(1)**, 1-17.

Moyer, M. J., and Kowalsky, M. J. (2003). "Influence of tension strain on buckling of reinforcement in concrete columns." *ACI Structural Journal*, **100(1)**, 75-85.

Pantazopoulou, S. J. (1998). "Detailing for reinforcement stability in RC members." *Jounal of structural engineering*, **124(6)**, 623-632.

Rodriguez, M. E., Botero, J. C., and Villa, J. (1999). "Cyclic stress-strain behavior of reinforcing steel including effects of buckling." *Journal of Structural Enginerring*, **125(6)**, 605-612.

Yalcin, C., and Saatcioglu, M. (1999). "Inelastic analysis of reinforced concrete columns." *Computers and structures*, **77(2000)**, 539-555.